

How are fine sediments described in sediment sheet flow?

Taro Uchida^{1*}, Yuki Nishiguchi², Satoshi Niwa³, Takeshi Kubo⁴, Yutaka Gonda⁵, and Yoshifumi Satofuka⁶

¹Faculty of Life and Environmental Sciences, University of Tsukuba, Tsukuba, Ibaraki, 3058572, Japan

²CTI Engineering, Co., Ltd., Tsukuba, Ibaraki, 3002358, Japan

³Japan Conservation Engineers, Co., Ltd., Urawa, Saitama, 3300074, Japan

⁴Kokusai Kogyo, Co., Ltd., Fuchu, Tokyo, 1830057, Japan

⁵Faculty of Agriculture, Niigata University, Niigata, 9502181, Japan

⁶College of Science and Engineering, Ritsumeikan University, Kusatsu, Shiga, 5258577, Japan

Abstract. Stony debris flow transits to sediment sheet flow when the river bed gradient becomes gentle. The sediment sheet flow consists of a water flow layer and a sediment moving layer. Fine sediments are expected to behave as a part of the fluid rather than a solid phase in the sediment moving layer. Further, it can be thought that a part of fine sediment can be suspended in the water flow layer. However, it was not possible to physically express whether the fine sediment behaves as a solid phase or a fluid phase in the numerical simulation model. Here we physically modeled fine sediment behavior in sediment sheet flow. We confirmed the applicability of the new model to describe the longitudinal deposited sediment gradient in flume experiments.

1 Introduction

A variety of flow types have been observed in mountain streams and laboratory experiments [1, 2]. Furthermore, several classifications have been proposed in terms of sediment concentration, flow velocity, grain size, and so on. In recent decades, several researchers have clarified that the thickness of the sediment moving (mixture) layer is one of the key characteristics of flow in mountain streams [3, 4]. In gentle streams with relatively coarse sediment, normal flow with bed load was commonly observed (Fig. 1a) [3, 4].

Several flume experiments demonstrated that the thickness of the sediment moving layer increases as the riverbed gradient increases (Fig. 1) [3, 4]. If the riverbed's critical value was exceeded, the sediments were distributed uniformly throughout the entire flow depth (Fig. 1c). This was referred to as "(stony) debris flow" [3]. If the riverbed gradient was less than the critical value, the sediment moving layer would occur only in the lower part of the flow (Fig. 1b) [3, 4]. This type of flow was referred to as "immature debris flow," "sediment sheet flow," and so on [3].

Stony debris flows composed consists of two phases: solid (e.g., rocks, stones, etc) and fluid. In stony debris flow, relatively coarse sediments move in a laminar manner [3, 4, 5]. However, interstitial fluid behaves as a turbulent flow. Flume experiments also revealed that when the particle size of bed sediment decreases, turbulent suspension occurs [4, 6]. Thus, fine sediments are expected to behave as a fluid phase rather than a solid phase in stony debris flows. Suspended sediment influenced pore water pressure [2, 4, 7]. This process increased the bouyon force acting on coarse sediment while decreasing energy dissipation caused by sediment collisions [5, 7]. Several numerical simulation models have been created [8]. Several models have incorporated this fine sediment processes [7, 9, 10]. In recent studies, we successfully reproduced various

debris flow behaviors using these models [7, 10], demonstrating the importance of fine sediments in debris flow.

It is possible that even in sediment sheet flow, fine sediment in the sediment moving layer behaves as an interstitial fluid (type B in Fig. 2). Furthermore, if a large amount of fine sediment is included in the sediment sheet flow, a part of the fine sediment may be turbulently suspended in the surface water flow layer (type A in Fig. 2). However, fine sediment behavior is not fully understood in sediment sheet flow. Thus, in many cases, types A and B sediment are not directly described in physically-based models. Here we created new numerical simulation models to physically describe fine sediment behavior in sediment sheet flow and used them in flume experiments.

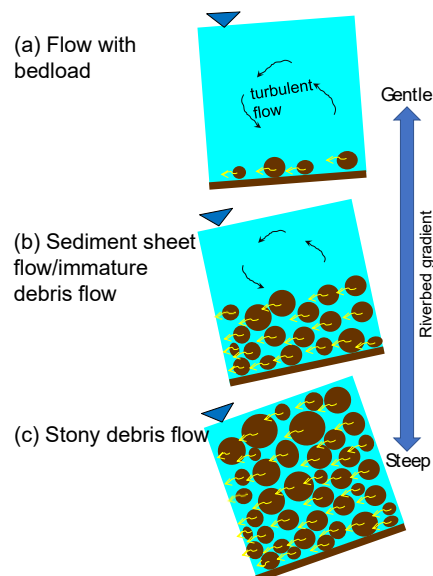


Fig. 1. Schematic illustration of flow type transition due to riverbed gradient change

* Corresponding author: uchida.taro.fw@u.tsukuba.ac.jp

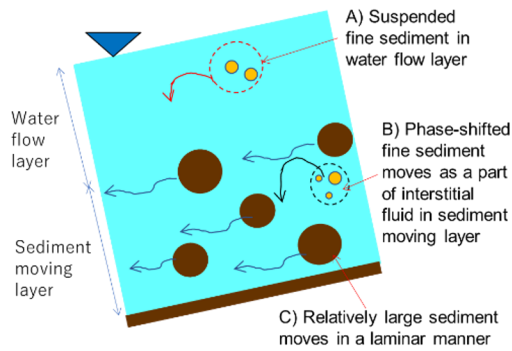


Fig. 2. Schematic illustration of sediment sheet flow

2 Flume experiments

We examined the sediment transport capacity of sediment sheet flow flume experiment data. The experimental flume was a straight rectangular channel 10 cm wide and 7 m long (Fig. 3). The flume's gradient was adjusted by 10 or 15 degrees. A 20-cm-high plate is installed at the downstream end of the flume. Then, we created a steady-state debris flow using a hopper and a pump. The equilibrium longitudinal gradient, defined as the gradient without bed erosion or deposition, was measured using three ultrasonic sensors. So, we can assess the sediment transport capacity under a given hydraulic condition.

We examined 56 experimental results in which the sediment concentration, water flow rate, flume gradient, and particle size distribution all varied (Table 1). The volumetric sediment concentration was set between 6.2 and 29.8 %. The water flow rate ranged from 0.75 to 2.5 L/s. In the experiments, four types of sand with varying particle size distributions and average diameters ranging from 1.03 to 3.62 mm were supplied from the hopper. The grain size distribution of used sand is shown in Fig. 4

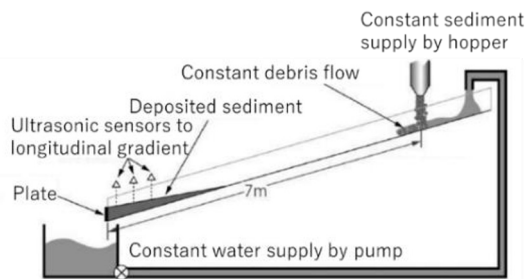


Fig. 4. Schematic illustration of flume experiments.

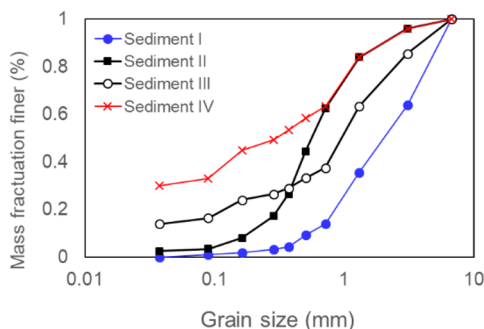


Fig. 5. Grain size distribution of sand for flume experiments

Table 1. Experimental condition

Case	Sediment	Gradient (deg.)	Water flow (ℓ /s)	Sediment conc. (%)
1	Sediment I	15	0.75	18.01
2		15	1	14.14
3		15	1.5	9.89
4		10	2	7.61
5		10	2.5	6.18
6		15	0.75	24.80
7		15	1	19.83
8		15	1.5	14.16
9		10	2	11.01
10		10	2.5	9.00
11		15	1	26.24
12		15	1.5	19.17
13		15	2	15.10
14		15	2.5	12.46
15	Sediment III	15	0.75	22.50
16		10	1	17.88
17		10	1.5	12.68
18		10	2	9.82
19		10	2.5	8.01
20		15	0.75	29.19
21		15	1	23.62
22		10	1.5	17.09
23		15	2	13.39
24		10	2.5	11.01
25		15	1	29.52
26		15	1.5	21.83
27		15	2	17.31
28		10	2.5	14.35
29	Sediment III	15	0.75	21.43
30		15	1	16.98
31		10	1.5	12.00
32		10	2	9.28
33		10	2.5	7.56
34		15	0.75	28.28
35		15	1	22.82
36		10	1.5	16.47
37		10	2	12.88
38		10	2.5	10.58
39		10	1	29.29
40		15	1.5	21.64
41		10	2	17.16
42		10	2.5	14.22
43	Sediment IV	15	0.75	21.24
44		15	1	16.82
45		15	1.5	11.88
46		15	2	9.18
47		15	2.5	7.48
48		15	0.75	26.85
49		15	1	21.59
50		10	1.5	15.51
51		15	2	12.10
52		15	2.5	9.92
53		15	1	29.82
54		15	1.5	22.07
55		15	2	17.52
56		15	2.5	14.53

3 Numerical simulation

3.1 Numerical simulation model

In this study, we developed a new numerical simulation model for describing three types of sediments in sediment sheet flow (types A through C in Fig. 2). The

followed the same trends as the theoretical relationship. While the difference between the data of sediment II through IV and the theoretical relationship was large, it suggested that the type C sediment could not fully describe the flume experiment results. This implies that if the effects of fine sediments are ignored, the equilibrium gradients should be overestimated in the case of sediments II through IV.

4.2 Comparison between flume experiment and numerical simulation

When we set $\alpha=3$, the calculated equilibrium longitudinal gradients agreed well with the observed equilibrium gradients (Fig. 7), even though the particle size distribution differed greatly. This implies that once we consider types A and B sediments and their effects, the equilibrium longitudinal gradients could be evaluated. Flume experiments revealed that the sediment concentration was two to three times higher than the theoretical values based on Takahashi's theory for type C sediments (dotted and broken lines in Fig. 6), implying that the roles of types A and B, as well as their effects on sediment transport capacity, maybe the same to two holds of type C.

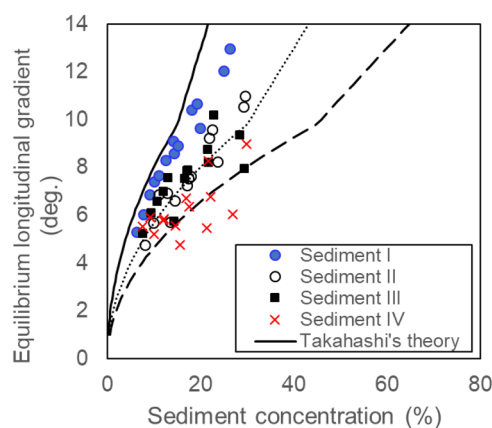


Fig. 6. Relationship between sediment concentration and equilibrium longitudinal gradient in flume experiments. The dotted and broken lines show the relationship when the sediment concentration doubles and triples concerning the sediment concentration at a certain gradient derived from Takahashi's theory.

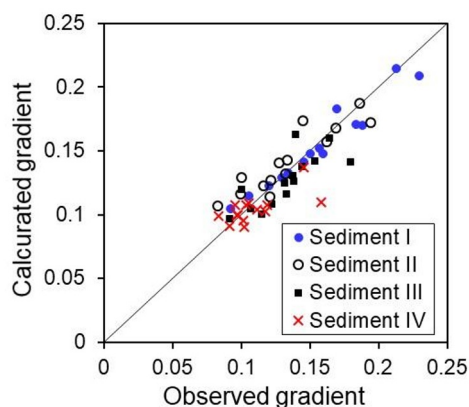


Fig. 7. Observed and calculated the longitudinal gradient of deposited sediment under steady condition

In this simulation, we searched best-fit α by trial and error. In suspended sediment theory, it has been generally assumed that sediments whose friction velocity exceeds their settling velocity will be suspended. While it has been reported that a part of the energy was dissipated by collision and friction of type C sediment in sediment sheet flow [1]. Thus, we believe that the $\alpha=3$ is reasonable.

5 Conclusions

We demonstrated that the transport capacity of sediment sheet flow cannot be described solely by sediment moving laminarly in the sediment moving layer. We must consider the effects of fine sediment suspended in a fluid to evaluate the transport capacity of sediment sheet flow. Here we proposed a simple method for a physical description of fine sediment behaviors in sediment sheet flow and developed a new numerical simulation model. Then, we used a new model to describe the equilibrium longitudinal gradient in flume experiments. We successfully described the relationship between sediment concentration, grain size distribution, and equilibrium longitudinal gradient, once we modeled fine sediment suspended in both the interstitial fluid of the sediment moving layer and the water flow layer.

References

1. B.W. McArdeall, *Int. J. Ero. Cont. Eng.*, **9**, 194-198 (2016).
2. R. Kaitna, M. Palucis, B. Yohannes, K. Hill, W.E. Dietrich, *J. Geophys. Res.*, **121**, 415-441 (2016).
3. T. Takahashi, *Debris flows*, (Taylor and Francis, London, 2007)
4. S. Egshira, *J. Disaster Res.*, **6**, 313-320 (2011)
5. R.M. Iverson, *Rev. Geophys.*, **35**, 245-296 (1997)
6. Y. Sakai, N. Hotta, K. Kaneko, T. Iwata, *J. Hydraul. Eng.*, **145**, 10.1061/(ASCE)HY.1943-7900.0001586 (2019)
7. T. Uchida, Y. Nishiguchi, B. McArdeall, Y. Satofuka, *Can. Geotech. J.*, **58**, 23-34 (2021)
8. M.G. Trujillo-Vela, A.M. Ramos-Canon, J. A. Escobar-Vargas, S.A. Galindo-Torre, *Earth-Sci. Rev.*, **232**, 104135 (2022)
9. R. Iverson, D. George, *PNAS*, **470**, 20130819, (2014)
10. T. Uchida, Y. Nishiguchi, K. Nakatani, Y. Satofuka, T. Yamakoshi, A. Okamoto, T. Mizuyama, *Int. J. Ero. Cont. Eng.*, **6**, 58-67 (2013)
11. Y. Nishiguchi, T. Uchida, *J. Geophys. Res.*, **127** 2021JF006452 (2022)
12. M. Hirano, H. Hashimoto, T. Teranaka, *Annual J. Hydraul. Eng.*, **41**, 759-764.